Accepted Manuscript

Composition dependence of structural and optical properties of $Cd_{1-x}Zn_xTe$ thick films obtained by the close-spaced sublimation

V. Kosyak, Y. Znamenshchykov, A. Čerškus, Yu P. Gnatenko, L. Grase, J. Vecstaudza, A. Medvids, A. Opanasyuk, G. Mezinskis

PII: S0925-8388(16)31391-3

DOI: 10.1016/j.jallcom.2016.05.065

Reference: JALCOM 37584

To appear in: *Journal of Alloys and Compounds*

Received Date: 12 February 2016

Revised Date: 25 April 2016

Accepted Date: 7 May 2016

Please cite this article as: V. Kosyak, Y. Znamenshchykov, A. Čerškus, Y.P. Gnatenko, L. Grase, J. Vecstaudza, A. Medvids, A. Opanasyuk, G. Mezinskis, Composition dependence of structural and optical properties of $Cd_{1-x}Zn_xTe$ thick films obtained by the close-spaced sublimation, *Journal of Alloys and Compounds* (2016), doi: 10.1016/j.jallcom.2016.05.065.

Composition dependence of structural and optical properties of $Cd_{1-x}Zn_xTe$ thick films obtained by the close-spaced sublimation

V. Kosyak[1,2], Y. Znamenshchykov[1 *], A. Čerškus[3], Yu. P.Gnatenko[4], L. Grase[2], J. Vecstaudza[2], A. Medvids[2], A. Opanasyuk[1], G. Mezinskis[2]

[1]Sumy State University, Rymskogo-Korsakova Str. 2, 40007 Sumy, Ukraine
[2]Riga Technical University, 3 Paula Valdena Str., LV-1048, Riga, Latvia
[3]Center for Physical Sciences and Technology, A. Gostauto Str. 11, LT-01108, Vilnius, Lithuania
[4]Institute of Physics of National Academy of Sciences of Ukraine, 03028 Kyiv, Ukraine

*E-mail: yaroslav.znamenshchykov@gmail.com

Abstract

This paper reports the results of structural, photoluminescence and Raman characterization of thick $Cd_{1-x}Zn_xTe$ films with different zinc concentration obtained by the close spaced vacuum sublimation method. The analysis of the X-rays patterns allows us to determine the effect of the zinc concentration on crystal quality of the films. It was found that samples with $x\approx0.10$ and $x\approx0.32$ have high crystal quality. However, with increasing of zinc concentration the crystal quality decreases. This result was confirmed by the photoluminescence study. Namely, the significant degradation of optical properties for the samples with high zinc concentration ($x>0.32$) was observed. Raman spectroscopy reveals the relation between zinc concentration and vibrational properties of the films. Also, the micro-Raman method shows that obtained films are uniform and free of tellurium inclusions.

Keywords: Crystal structure, Semiconducting ternary compounds, Lattice defects, X-ray diffraction, Photoluminescence, Raman spectroscopy.

1. Introduction

Due to the high atomic number, high density and adjustable band gap (BG) from 1.50 eV (CdTe) to 2.26 eV (ZnTe) [1] the single crystals of $Cd_{1-x}Zn_xTe$ (CZT) ternary semiconductor are widely used for hard radiation detectors [1–4].

It should be noted that the presence of zinc atoms substantially increases the resistivity of CZT crystals and hence their performance as a detector [4]. On the other hand, it may lead to decreasing in crystal quality due to lattice deformation [5–7]. Also,

the nonuniformity of Zn distribution in the crystal volume is one of the key problems of their growth technology [3,4,8,9]. This is the reason that for the most of CZT detectors the concentration of Zn atoms does not exceed 20% [3]. At the same time, theoretical calculation shows advantages in the use of CZT with Zn concentration up to 80% [10]. The necessity of obtaining the low-cost and large-area uniform CZT wafers for X-ray imaging detectors [11] lead to usage of thick films with the thickness of 30 μm [12,13] and more [11,14–17] instead of bulk crystals.

In addition, CZT films are used in photovoltaic applications as a top absorber layer in CIGS solar cells [18–20] or as a contact layer in CdTe solar cells [21]. Moreover, the possibility of elaboration of graded band gap solar cells based on CZT was also recently considered in [22].

Different methods such as metalorganic vapor-phase epitaxy [13], metal–organic chemical vapour deposition [7] pulsed laser deposition [23] thermal evaporation [15,17,24], brush plating technique [25], magnetron sputtering [26], hot wall epitaxy [14] were used for CZT films deposition. Among these methods, the close-spaced sublimation (CSS) can be considered as a very promising low-cost technique for obtaining of CZT layers which have high optical quality [27–29]. Usually, CSS growth is performed by the evaporation of CZT powder [27–30] or sequential deposition of elements [31,32]. Using co-evaporation of CdTe and ZnTe compounds could be a more promising approach, because one can expect a fine adjustment of Zn amount with the possibility to form a concentration gradient in order to obtain graded BG material.

X–ray diffraction (XRD) [7,8,24,31], low-temperature photoluminescence (PL) [6–8,33] and Raman spectroscopy [1,23,27,34,35] are the most useful characterization techniques to study CZT crystals and films, since these methods not only provide information about optical and crystal quality but also let us estimate Zn concentration.

Determination of Zn concentration using XRD data is based on Vegard's law which describes the linear dependence of $Cd_{1-x}Zn_xTe$ lattice constant on x [7]. The crystal quality of the samples was obtained using a full width at half maximum (FWHM) of the main (111) diffraction peak [7,8].

PL properties of CZT crystals, especially in the case of low Zn concentration, are well studied [4,36,37]. Usually, the broad defect band, donor-acceptor transitions bands and excitonic luminescence lines are observed in PL spectra [36,38]. The BG value (E_g) is determined from the energy position of excitonic emission lines [39]. The relationship between Zn concentration and the value of E_g was determined experimentally and theoretically [6,39,40], that let us use of PL measurements as an effective method for determination of Zn amount in CZT solid solution.

The study of CZT compound by using Raman scattering (RS) spectroscopy is based on an analysis of the phonon spectra [1,35]. General properties of CZT RS spectra are well described in [1,23,34,41]. As a rule, the RS spectra include CdTe- and ZnTe-like longitudinal (LO) and transverse (TO) optical phonons modes. The RS spectroscopy is very sensitive to the presence of Te inclusions in CZT. Thus strong Te-related modes also could be detected [23,25,33]. The relation between the energy position of (LO) and (TO) lines and zinc concentration was determined in [23,34,35,41]. The crystal quality of samples could be estimated according to the presence and intensity of phonon replicas [35,42].

For different applications, the key problem of CZT films technology is the obtaining of high-quality layers with the pre-specified Zn concentration as well as its distribution even in the case of Zn-rich samples.

Thus, the main objective of this paper is a comprehensive study of structural and optical properties of $Cd_{1-x}Zn_xTe$ thick films with different concentrations of Zn atoms and analysis their spatial distribution in order to obtain the thick films of high optical quality for the Zn concentrations of $x>0.10$.

2. Materials and methods

The CZT thick films were obtained by close-spaced vacuum sublimation (CSVS) analogously as in our previous works [43–45] in the case of the CdTe deposition. Taking into account the ternary compound, the setup of films growth was equipped with two independent evaporators for CdTe and ZnTe materials. The stoichiometric CdTe and ZnTe powders were placed separately into different evaporators without mixing. In order to obtain CZT films with different Zn concentration the mass ratio (M_R) between CdTe to ZnTe powders has been varied as follows: 8, 4, 3 and 2 for CZT1, CZT2, CZT3 and CZT4 samples, respectively. Also, thick films of the pure CdTe and ZnTe compounds were obtained by CSVS method. The diameter of the samples was 1.6 cm. The growth conditions of different films were same, namely, the substrate temperature was 400 ^{0}C, temperature of the CdTe and ZnTe evaporators was 620 and 700^{0}C, respectively. The ultrasonically cleaned Mo-coated glass slides were used as substrates.

The microstructure of the CZT films was studied by FEI Nova NanoSEM 650 Schottky field emission scanning electron microscope (SEM) with an integrated Apollo X energy dispersive spectroscope (EDS) for the chemical composition analysis using standardless energy techniques. The following parameters of EDS experiment were used: accelerating voltage 15 kV, detector resolution 125.4 eV, working distance 7 mm and spot size 5.5.

Structural analysis was carried out by Rigaku Ultima+ X-ray diffractometer using KαCu radiation source, the scan step was 0.003 2-theta degrees.

The PL measurements were performed using a standard setup with a fully automated 1-m focal length monochromator. The excitation was provided by 457 nm (2.71 eV) CW diode pumped solid state laser. The diameter of the laser spot was about 1 mm. The excitation intensity was reduced to 9 W/cm^2 using neutral glass filters. The PL spectra were dispersed using a blazed at 750 nm holographic grating of 1200 mm^{-1}, achieving the spectral dispersion of 0.8 nm/mm. The PL spectra were obtained by a thermoelectrically cooled, high efficiency extended-red multi-alkali cathode photomultiplier operating in the photon counting regime. The sample temperature could be varied from room temperature (300 K) down to 3.6 K using a closed cycle helium optical cryostat.

Room temperature RS spectra were studied using Renishaw InVia 90V727 micro-Raman spectrometer in a backscattering geometry using 1200 and 1800 mm^{-1}grating for the semiconductor IR (λ=785 nm), HeNe (λ=633 nm) and an Ar (λ=514 nm) laser excitation, respectively. Registration of signal was carried out by CCD camera. Calibration of the spectrometer was done by measuring Raman line at 520 cm^{-1} of the silicon wafer. The power of excitation was set as a percentage of the nominal power of 25 mW, 12.5 mW, 300 mW for the green Ar, red HeNe, semiconductor IR lasers, respectively. The diameter of the laser spot is dependent on wavelength of the laser radiation, and it was calculated to be 0.7, 0.9 and 1.1 µm for the green, red and IR lasers, respectively. The accumulation time and power of excitation were chosen so as to obtain high signal-to-noise ratio while avoiding damage of the surface and high background luminescence.

3. Results and discussion

3.1 Surface and EDS analysis

The SEM images of the CZT samples are presented in Fig.1. As can be seen, the decreasing in the mass ratio between CdTe and ZnTe powders leads to significant modification of the surface of deposited films. Namely, the CZT1 sample consists with quite uniformly distributed grains with the average size (*D*) of 8 µm. While, the surface of CZT2 sample is less uniform. Also, the value of *D* decreases down to 5 µm. This value for CZT3 sample is very similar to CZT2 whereas most grains show subgrains of about 1 µm size. The surface of CZT4 sample is composed of layered-like crystallites with irregular shapes and *D* value of 7 µm. Such degradation of the surface could be explained by the deterioration of the crystal lattice due to increasing amount of Zn

atoms. Another possible explanation is related to technological features of CZT deposition by CSVS. We assume that CZT samples were obtained under growth condition which is more favorable for CdTe than ZnTe films, since the difference between the evaporator and substrate temperatures $\Delta T=T_e-T_s$, is 220 ^{0}C and 300 ^{0}C for CdTe and ZnTe respectively. Thus, the Zn-poor films were grown under more equilibrium condition than Zn-rich samples.

The thicknesses of the samples were measured by SEM from the samples cross-section and were about 30 µm.

The results of EDS spectroscopy are presented in Table 1. As follows from Table 1, the concentration of Zn atoms increases with M_R decrease.

3.2 XRD analysis

The XRD patterns measured for the CdTe, ZnTe samples (Fig.2) shows peaks from (111), (200), (220), (311), (400), (331), (422) and (511) planes of the cubic zinc blende phase [43,46]. The same peaks were detected on XRD spectra of the CZT samples which suggest that formation of the solid solution does not change phase composition of films. At the same time, the peaks in XRD patterns of the CZT1÷CZT4 films are shifted toward higher degrees relatively to peak positions in CdTe because of increasing in Zn content. The values of Zn concentration were determined by the Vegard's law [7] using calculated lattice parameter (Table 1). The numerical values of x are presented in Table 1. As can be seen from Table 1 the Zn concentration is expectedly increased with a decrease in M_R. Some disagreement between x values obtained from EDS and XRD study is observed. We suppose that this is due to the fact that accuracy of EDS measurements of non-polished samples with a high surface roughness could be more than 5% [47]. Also, it could be because of some through-thickness inhomogeneity in Zn concentration of the CZT samples. This explanation seems reasonable because the XRD method provides integral information about Zn concentration in CZT films, whereas EDS method is limited by the penetration depth of X-ray probe, which is approximately a few µm.

It is well known that in the range from x=0 to 1 the relationship between Zn concentration and the value of FWHM of the (111) peak of CZT can be described by a parabola with the maximum near x=0.5 [6,7]. This reflects high deformation of the crystal lattice of the CZT solid solutions comparatively with the pure CdTe and ZnTe compounds. In general, we observed such effect in our study. Namely, the FWHM of the (111) peak is higher for CZT samples than for CdTe and ZnTe (Table 1) and it monotonically increases with x. One can expect some improvement in the crystal quality of the CZT4 sample in comparison with CZT3 sample. In this case, x value of 0.44 for

CZT3 sample suggests maximal deformation of crystal lattice among all investigated samples. However, the FWHM of the (111) peak for CZT4 sample is about twice higher than for CZT3 sample. This could be explained by the difficulties in obtaining of very Zn-rich CZT thick films with uniform Zn distribution by CSVS method. Thus, we assume that CZT4 sample includes several sublayers with the different Zn concentration. At the same time, the very broad (111) peak of CZT4 sample is due to overlapping of the few diffraction peaks from such sublayers.

Calculations of coherent scattering domains (CSD) size and microstrains (MS) by the method described in [48,49] confirm decreasing of crystal quality with increasing in Zn concentration (Table 1).

3.3 Photoluminescence studies

The low-temperature PL measurements [50–52] let us determine the nature and energy levels of both the intrinsic defects and the residual impurities as well as the relative concentration of dislocations in semiconductor materials [53,54]. In this case, the excitonic PL lines are very sensitive to various defects in semiconductors. The excitation energy of free excitons (bound electron-hole pairs) is slightly less than the band gap energy E_g of semiconductors. Usually, strong lines caused by the bound excitons (BE) appear in the low-temperature PL spectra for semiconductors of high optical quality. It should be noted that the energy of BE is less than the energy of free exciton by the amount equal to its energy binding and depends on the nature of the impurity or intrinsic defects. So, the energy position of the BE determines the nature of the defects participating in the formation of the excitonic complexes. In the case of semiconductor alloys, crystal potential field fluctuations (CPFFs) occur due to random distribution of component composition [55–57]. Excitonic states are localized at these fluctuations and the low-energy tails in the density of excitonic states arise [58,59]. The energy position of the localized excitons (LE) is shifted to the low-energy region relative to the energy of free excitons by the amount corresponding to the energy about 1/2 of the full width at half maximum (FWHM) of the LE band [60]. Taking into account the binding energy of free exciton for CdTe and ZnTe crystals, which corresponds to about 10 meV, we can determine the band gap of the semiconductor crystals (or films).

Thus, for semiconductor alloys, the excitons are localized both near point defects and at CPFFs, which reflects inhomogeneity of their composition. The manifestation of LE is fairly well studied for bulk II-VI compounds. It should be noted that PL exciton lines for thin and thick semiconductor films usually are identified only as PL lines, caused by excitons bound with donor or acceptor centers. Thus, in this case, the formation of LEs associated with the presence of a strong heterogeneity in the distribution of component composition is not considered. Analysis of the PL spectra

presented below takes into account the presence in $Cd_{1-x}Zn_xTe$ as bound and localized excitons.

PL spectra of the films obtained for CdTe, ZnTe and CZT1-CZT4 samples are shown in Fig. 3. In this case, CdTe and ZnTe samples were obtained by CSVS method under growth conditions similar to $Cd_{1-x}Zn_xTe$ films. It should be noted that these CdTe and ZnTe materials were used for the deposition of the films.

PL spectrum for CdTe thick film is shown in Fig. 3a. The intense excitonic emission at E=1.591 eV, which is associated with the recombination of excitons bound on a neutral acceptor (A^0X-line) with the participation of cadmium vacancy (V_{Cd}), is observed in the PL spectra [61]. Since the binding energy of BE (A^0X-line) is equal ~5 meV [43], the band gap of CdTe sample is equal to 1.606 eV that coincides with the corresponding value for bulk CdTe. The presence of intense excitonic line indicates a fairly good optical quality of the investigated semiconductor films [62]. The PL band at 1.547 eV is caused by the recombination of free electrons and acceptor centers ((e,A)-transition) [1,14]. By knowing the energy of this PL line and the value of E_g (4.5 K) = 1.606 eV for CdTe film, we can determine the energy of the acceptor level as it was done in [54]. Thus, we obtain the energy of the acceptor center associated with (e,A)-transition, namely E_A= 59.0 meV. This value is close to the acceptor energy of Li or Na (58.0 meV and 58.7 meV, respectively) [63]. The energy of both these exciton acceptor complexes is about 1.589 eV [63]. This indicates that in addition to cadmium vacancies, there exist other acceptor centers in CdTe sample. However, the intensity of A^0X-line is mainly determined by the emission from the exciton complex involving cadmium vacancy.

The broad band at 1.495 eV can be caused by the donor-acceptor pairs (DAP) recombination with the participation of complexes (V_{Cd} – D), where D is residual donor (atoms of III or VII group metals). The difference between the value of E_g=1.606 eV (T=4.5 K) for CdTe and the peak position of the band is equal to 111 meV. The energy of the shallow donor in CdTe is equal to 14 meV [64]. Using these parameters analogously to [54] we obtained the energy of the acceptor center, which participates in the DAP emission, namely 117 meV. This energy is close to the energy of Ag acceptor center (107 meV) [63]. In the PL spectrum, another intense PL band at 1.477 eV and its 1LO- and 2LO-phonons replicas are observed at 1.456 and 1.435 eV, respectively. In this case, the energy of LO-phonon is about 21 meV. According to [65–68] the PL band at 1.477 eV is due to Y center which corresponds to excitons bound on Te glide dislocations. Thus, the intensity of the Y band may be used as an indicator of the presence of dislocations in CdTe.

The intense exciton emission line at 1.653 eV is observed in the PL spectrum for $Cd_{1-x}Zn_xTe$ (CZT1 sample), which is shown in Fig. 3b. This PL line is mainly caused by the recombination of excitons bound on a neutral acceptor (A^0X-line). It is found that the value of E_g for CZT1 sample is equal to 1.668 eV at T=4.5 K. It should be noted that this line has high-energy asymmetry that can be caused by some overlapping of A^0X-line with the lines of localized excitons appearing on its high-energy wing. Another line at 1.619 eV is due to the (e,A)-transition with the participation of the cadmium vacancy acceptor which has its energy equal to 49.0 meV. The FWHM of this line is smaller than that for CdTe sample. We assume that in the latter case other acceptors with different ionization energies are involved in these optical transitions. This may be the residual impurities such as Li, Na, N and P with the energies of 58.0, 58.7, 56.0 and 68.2 meV [63]. As can be seen from Fig. 3b, the 1LO-phonon replica of (e,A)-transition is observed at 1.597 eV. Another very broad PL band at 1.497 eV corresponds to so-called D PL band, caused by the presence of point and extended defects of dislocation type as well as microstrains in the films [66,69].

In Fig. 3c, the PL spectrum for CZT2 sample is shown. Similar to the previous film sample, the most intensive line is the exciton line at 1.820 eV. It should be noted that its FWHM is equals to 24 meV, i.e. it practically coincides with the similar value for CZT1 sample (23 meV). It is obvious that the rising of Zn concentration above x=0.10 leads to the increasing of the contribution of the LE. Thus, for CZT2 sample, the emission of the LE is dominant in the PL spectrum. Taking into account the energy value of 1/2 FWHM which is equal of 12 meV for the LE we determine the band gap for CZT2 sample which corresponds to 1.842 eV. The PL spectrum also includes other broad bands at 1.778, 1.657 and 1.593 eV. The first band may be caused by (e,A)-transition, where the acceptor energy is equal to 64 meV and can correspond to the ionization energy of residual impurities (Li, Na and P) [63]. It is obvious that the PL bands at 1.657 and 1.593 eV correspond to the emission of DAP with the participation of A-centers and D band associated with the presence of dislocations.

For CZT3 sample, the high-energy PL line, shown in Fig. 3d at 1.974 eV, also corresponds to the recombination of LE. Taking into account the energy value of 1/2 FWHM for this exciton line (12 meV), we can determine the value E_g, which is equal to 1.996 eV. The other PL band at 1.921 eV may be caused by the recombination of DAPs with participation of donor and acceptor centers with the energies of 14 meV and 61 meV. The last energy is close to the energy of the Li or Na acceptors. The broad PL bands at 1.872 and 1.817 eV correspond to the DAP recombination and the emission of Y-band, respectively. Therefore, it is expected that the energy of acceptor center is about 110 meV, which is close to the energy of Ag acceptor center (107 meV) [63].

In Fig. 3e the PL spectrum for CZT4 sample with the highest concentration of zinc atoms is shown. In this spectrum, there exists emission in the spectral region, which is characteristic to CdTe film. In particular, the line at 1.585 eV is very close to the energy position of (A^0X)-line in CdTe. Other line at 1.546 eV may be caused by (*e*,*A*)-transition. The emission at 1.495 eV also coincides with the recombination of DAP similar to CdTe. The broadening of these lines is caused by the presence of high concentration of microstrains in the investigated sample. This is also supported by the presence of a very broad band at 1.796 eV, which is most likely related to the emission with the participation of various extended defects, especially dislocations. In the high-energy spectral range the strongly blurred PL band is observed at the energy of about 2.100 eV. This band can be determined as strongly broadened line of LE with the value of 1/2 FWHM, approximately 40 meV. Thus, the band gap for Zn-rich region film of CZT4 sample can be equal to about 2.150 meV.

The line with the highest energy at 2.365 eV for ZnTe sample shown in Fig. 3f, corresponds to A^0X-line and is caused by the zinc vacancy acceptor exciton complex [70]. The energy position of free exciton in ZnTe films corresponds to 2.384 eV [70]. Since the binding energy of free exciton is 11 meV, the band gap of ZnTe film is equal of 2.395 eV. The most intensive line at 2.317 eV is caused by the emission of DAP's and is the zero-phonon line. Other lines observed on the long-wavelength part of the spectrum are 1LO and 2LO-phonon replicas of the line at 2.29 and 2.27 eV, respectively. The broad band at 1.622 eV is caused by the emission with participation of deep impurity level.

3.4 Raman spectra

The optimal conditions (power and wavelength of excitation, accumulation time) for Raman scattering (RS) measurements should be chosen in such a way to provide the good quality of spectra suitable for reliable analysis. The high signal-to-noise ratio is achieved under resonant conditions when the energy of incoming photons E_{in} is close to fundamental valence-to-conduction band E_0 gap [23,34,71]. For CdTe and ZnTe crystals at room temperature this value corresponds to the energy of 1.51 and 2.27 eV, respectively [72]. For example, the authors of the works [23,34] suggest adjusting of the energy of excitation radiation slightly above fundamental valence-to-conduction band. Thus, in a case of RS study of the CZT films with variable Zn concentration in [23], the wavelength of laser excitation was decreased with increasing Zn concentration. Namely, infrared (755 nm), red (647 nm) and green (514 nm) radiations were used for excitation of CdTe, CZT and ZnTe samples, respectively. It should be noted that under the resonant conditions the high background luminescence could influence the Raman

spectra since the excitation wavelength is close to the band gap of the material. Raising background makes an analysis of the spectra more complex [73,74] and can lead to overflow of the detector.

The resonance conditions are also observed if E_{in} is close to spin-orbit-split-off gap $E_0+\Delta_0$ [74] ($E_0+\Delta_0$ = 2.41 eV for CdTe at room temperature [72]), so called incoming resonance, or if following condition $E_{in}-m\hbar\omega_{LO}\approx E_0+\Delta_0$ is satisfied for incoming photon with energy E_{in} which is scattered m times by LO phonon with frequency ω_{LO} ($m\hbar\omega_{LO}$=21.2 meV for CdTe at temperature of 2 K [74]), i.e. outgoing resonance [74].

It is very important to avoid local overheating of the material which may lead to misinterpretation of the obtained results. The green excitation with a high energy is often used for the Raman study of the CdTe and CZT samples with low Zn concentration [33,75,76]. The energy of green or blue wavelength radiation is much higher than BG of CdTe or Zn-poor CZT and hence, the high absorbance of excitation radiation occurs. In this case, the penetration depth of the green wavelength radiation for CdTe and ZnTe is only 200 and 400 nm, respectively [75]. Thus, the excitation light is absorbed in a thin near-surface layer that could lead to local heating of the material followed by Te enrichment on the surface, even at low green laser excitation power [75,77,78]. In order to determine the position of Te-related modes, the tellurium crystal was measured as a reference, using three available laser excitations wavelengths. As could be seen from Fig.4 the good spectra for all excitation wavelengths even with low excitation power and small accumulation time were obtained. It should be noted that accumulation time of 20 sec was the same for three excitation wavelengths while excitation power density was 67, 8 and 6 W/cm^2 for 514, 633 and 785 nm lasers, respectively. The measured RS spectrum of Te crystal (Fig.4) shows typical strongest features due to A_1 symmetry phonon at 123 cm^{-1} and two E_{TO} modes at 95 and 143 cm^{-1} [76].

Further, to determine the optimal conditions for RS measurements, three laser excitation wavelengths were used for pure CdTe. The results of RS measurements of CdTe sample are presented in Fig.5. It is found that the spectrum of CdTe sample (Fig.5a) which obtained during 1200 sec with 514 nm (E=2.41 eV) excitation and 33.9 W/cm^2 power density includes only CdTe-related modes, namely, TO_1 mode at 141 cm^{-1} as well as LO_1 mode at 166.5 cm^{-1} and its $1LO_1$ and $2LO_1$ replicas at 330 and 500 cm^{-1}, respectively [1,34,35,74,76]. It should be noted that according to selection rules for the zinc-blende structure the (111) crystal orientation of the polycrystalline films allows the presence of CdTe-like TO_1 mode [76]. In contrast to (100) crystal orientation when TO_1 mode is forbidden [34,76]. The excitation energy of 2.41 eV satisfies resonance conditions with spin-orbit-split-off gap $E_0+\Delta_0$=2.41 eV as mentioned above. However,

in this case, only $1LO_1$ and weak $2LO_1$ phonon replica were observed, whereas resonance RS spectra usually include higher order overtones [74]. Also, the obtained spectrum is quite noisy that may indicate the absence of resonant enhancement of Raman signal. The attempt to improve spectrum quality by increasing of laser power density to 678 W/cm^2 has led to the appearance of strong Te-related A_1 and E_{TO} modes. Here CdTe-related TO_1 mode cannot be reliably identified due to overlapping with Te-like E_{TO} line. We assume that the appearance of the strong Te-related modes is caused by local heating of the sample surface, as this was shown in [75,77,78].

This assumption was confirmed by RS measurement using 633 nm excitation wavelength. As could be seen from Fig.5b the RS spectrum includes only CdTe-related LO_1 and TO_1 modes. In this case, the measurement was carried out at low excitation power density of 3.44 W/cm^2 and accumulation time was only 20 sec that practically excluded local heating of the material.

The spectrum with best signal-to-noise ratio is shown in Fig.5c. This spectrum was obtained using IR excitation with 785 nm wavelength (E=1.579 eV). As well as in the case of measurements with 633 nm, the excitation with 20 sec accumulation time was used while excitation power density of 0.67 W/cm^2 was smaller. The value of incoming excitation energy is close to fundamental band gap and the resonant Raman spectrum was observed. In particular, $1LO_1$, $2LO_1$ and $3LO_1$ replicas were detected (Fig.5c). Thus, the RS study of pure CdTe sample suggests application of IR (E=1.579 eV) excitation for the resonant enhancement of the RS signal of CZT1 sample with comparatively low zinc concentration (x=0.10) since the value of BG at room temperature for this sample is about 1.57 eV [39]. At the same time, the 633 nm excitation (E=1.958 eV) is more suitable for wider band gap CZT2, CZT3, CZT4 and ZnTe samples. For these measurements we used small accumulation time of 20 sec and low power excitation of 0.67 W/cm^2 as well as 0.60 W/cm^2 for red and infrared excitation, respectively.

The results of measurements of CZT1-CZT4 samples using mentioned above laser excitations are presented in Fig.6. According to the works [34,35,41] positions of ZnTe and CdTe-like modes in RS spectra of CZT are shifted from those in pure compounds depending on Zn concentration. In particular, the CdTe-like LO_1 mode is blue-shifted from the position of LO_1 for pure CdTe (167 cm^{-1}), while CdTe-like TO_1, ZnTe-like LO_2 and ZnTe-like TO_2 modes are red-shifted [34,35]. In general, such trend was observed in the present study. As could be seen from Fig.6 the spectrum of CZT1 sample includes two peaks at 162 and 178 cm^{-1} which were assigned to be CdTe –like LO_1 and ZnTe-like LO_2 modes, respectively, as well as their resonant overtones $1LO_1$ and $1LO_2$. Thus, the RS spectrum of CZT1 sample shows two-mode behavior similar to

the works [34,35]. The spectra of CZT2, CZT3 and CZT4 samples show an increasing shift of LO_2 toward the position of this mode at 206 cm^{-1} for pure ZnTe, the values of Raman shift of LO_2 mode for CZT and ZnTe samples are listed in Table 1. Low-intensity ZnTe-like TO_2 mode appears on the RS spectra of CZT2-CZT4 Zn-rich samples, and this mode is slightly red-shifted. While on the RS spectra of CZT1 and CZT2 samples the LO_1 mode is blue-shifted from the position of LO_1 mode for CdTe. It should be noted that intensities of CdTe-like modes are decreased with increasing Zn concentration. Moreover, LO_1 is not observed on the spectra of Zn-rich CZT3 and CZT4 samples, and only RS spectrum from pure CdTe sample shows weak CdTe-like TO_1 peak. The spectrum of ZnTe sample includes dominant LO_2 mode and much less intensive TO_2 at 177 cm^{-1}, as well as transversal acoustic mode TA at 109 cm^{-1} and its combination with LO_2 at 241 cm^{-1}, i.e. TA+LO_2 [79].

It should be noted that scanning of the surface of CdTe, ZnTe and CZT samples by micro-Raman did not reveal any changes in values of Raman shift for the main modes CdTe or ZnTe-related modes across the surface. It means that surface distribution of compound elements in samples is uniform. Also, the Te-inclusions were not detected in any sample.

4. Conclusions

The study of CZT samples by XRD, PL and Raman spectroscopy show that CSVS method allows obtaining sufficiently uniform and high-quality thick films with Zn concentration up to 30%. Further increasing in Zn concentration leads to a gradual decrease in crystal quality of films. In particular, the generally accepted for the $Cd_{1-x}Zn_xTe$ parabolic behavior of crystal quality vs Zn concentration relationship, when x is changed from 0 to 1, was not confirmed by PL and XRD experiments. This was explained by the fact that Zn-poor films were obtained under more equilibrium growth condition that Zn-rich films, since the difference between evaporator and substrate temperatures ΔT, for CdTe (ΔT=220 ^{0}C) is less than for ZnTe (ΔT=300 ^{0}C). In other words, we observed the effect of non-optimal growth conditions on crystal quality of Zn-rich CZT samples rather than typical for the bulk material relationship between deformation of the crystal lattice and Zn concentration. Thus, we suppose that improvement of the crystal quality of Zn-rich CZT films is possible by the gradual increasing of substrate temperature in order to decrease ΔT and provide growth conditions similar to the deposition of pure ZnTe.

The PL spectra of CdTe, ZnTe and Zn-poor CZT1 and CZT2 samples show most intense A_0X line appeared due to the low recombination of acceptor bound excitons with the participation of cadmium vacancy. The presence of intense excitonic line indicates a

fairly good optical quality of these samples. In a case of Zn-rich $Cd_{1-x}Zn_xTe$ samples, the broad PL bands caused by dislocations became dominant while relative intensity of A_0X line significantly decreased.

It was established that application of high power excitation laser during Raman spectroscopy experiment may lead to the formation of Te-rich surface and hence to misinterpretation of the results of the phase analysis. Thus, it is possible to conclude that resonant conditions, when high noise-to-signal ratio could be achieved even at low power of excitation laser radiation, are optimal for Raman measurements. It was shown that concentration behavior of the CdTe and ZnTe-like Raman modes is well correlated with commonly accepted theory of optical phonon in $Cd_{1-x}Zn_xTe$ solid solution. The micro-Raman method shows that CSVS method is suitable for obtaining of high-quality CZT films free of Te inclusions.

Acknowledgments

This work was supported by Erasmus Ianus Programme and by the Ministry of Education, Science of Ukraine (Grant No. 0115U003242, 0113U000131) by the National Academy of Sciences of Ukraine (Grants Nos. BC-157-15 and B-146-15) and State Fund for Fundamental Research (project N GP/F61/087).

References

[1] R. Triboulet, P. Siffert, CdTe and Related Compounds; Physics, Defects, Hetero- and Nano-structures, Crystal Growth, Surfaces and Applications, Elsevier, Amsterdam, 2010.

[2] A. Owens, Compound Semiconductor Radiation Detectors, CRC Press, Boca Raton, 2012.

[3] S. del Sordo, L. Abbene, E. Caroli, A.M. Mancini, A. Zappettini, P. Ubertini, Progress in the development of CdTe and CdZnTe semiconductor radiation detectors for astrophysical and medical applications, Sensors. 9 (2009) 3491–3526.

[4] M. Fiederle, T. Feltgen, J. Meinhardt, M. Rogalla, K.W. Benz, State of the art of (Cd,Zn)Te as gamma detector, J. Cryst. Growth. 197 (1999) 635–640.

[5] M.E. Rodríguez, J.J. Alvarado-Gil, I. Delgadillo, O. Zelaya, H. Vargas, F. Sánchez-Sinencio, et al., On the Thermal and Structural Properties of $Cd_{1-x}Zn_xTe$ in the Range $0 < x < 0.3$, Phys. Status Solidi. 158 (1996) 67–72.

[6] J.L. Reno, E.D. Jones, Determination of the dependence of the band-gap energy on composition for $Cd_{1-x}Zn_xTe$, Phys. Rev. B. 45 (1992) 1440–1442.

[7] S. Stolyarova, F. Edelman, A. Chack, A. Berner, P. Werner, N. Zakharov, et al., Structure of CdZnTe films on glass, J. Phys. D. Appl. Phys. 41 (2008) 065402.

[8] J.Pérez Bueno, M. Rodríguez, O. Zelaya-Angel, R. Baquero, J. Gonzalez-Hernández, L. Baños, et al., Growth and characterization of $Cd_{1-x}Zn_xTe$ crystals with high Zn concentrations, J. Cryst. Growth. 209 (2000) 701–708.

[9] A. Mychko, A. Medvid, E. Dauksta, Laser-induced increase of resistivity and improvement of optical properties of CdZnTe crystal, J. Cryst. Growth. 415 (2015) 47–50.

[10] J.E. Toney, T.E. Schlesinger, R.B. James, Modeling and Simulation of Uniformity Effects in Cd_{1-x} Zn_xTe Gamma-Ray Spectrometers, IEEE T Nucl Sci. 45 (1998) 105–113.

[11] P.J. Sellin, Thick film compound semiconductors for X-ray imaging applications, Nucl. Instruments Methods Phys. Res. Sect. A Accel. Spectrometers, Detect. Assoc. Equip. 563 (2006) 1–8.

[12] S. Kang, B. Jung, S. Noh, C. Cho, I. Yoon, J. Park, Feasibility study of direct-conversion x-ray detection using cadmium zinc telluride films, J. Instrum. 7 (2012) C01010.

[13] M. Niraula, K. Yasuda, S. Namba, T. Kondo, S. Muramatsu, Y. Wajima, et al., MOVPE Growth of Thick Single Crystal CdZnTe Epitaxial Layers on Si Substrates for Nuclear Radiation Detector Development, IEEE Trans. Nucl. Sci. 60

(2013) 2859–2863.

[14] J. Takahashi, K. Mochizuki, K. Hitomi, T. Shoji, Growth of $Cd_{1-x}Zn_xTe$ (x=0.04) films by hot-wall method and its evaluation, J. Cryst. Growth. 269 (2004) 419–424.

[15] K. Kim, S. Cho, J. Seo, J. Won, J. Hong, S. Kim, Type conversion of polycrystalline CdZnTe thick films by multiple compensation, Nucl. Instruments Methods Phys. Res. Sect. A Accel. Spectrometers, Detect. Assoc. Equip. 584 (2008) 191–195.

[16] S. Tokuda, H. Kishihara, S. Adachi, T. Sato, Preparation and characterization of polycrystalline CdZnTe films for large-area, high-sensitivity X-ray detectors, J. Mater. Sci. Mater. Electron. 15 (2004) 1–8.

[17] J.H. Won, K.H. Kim, J.H. Suh, S.H. Cho, P.K. Cho, J.K. Hong, et al., The X-ray sensitivity of semi-insulating polycrystalline CdZnTe thick films, Nucl. Instruments Methods Phys. Res. Sect. A Accel. Spectrometers, Detect. Assoc. Equip. 591 (2008) 206–208.

[18] S.H. Lee, A. Gupta, S. Wang, A.D. Compaan, B.E. McCandless, Sputtered $Cd_{1-x}Zn_xTe$ films for top junctions in tandem solar cells, Sol. Energy Mater. Sol. Cells. 86 (2005) 551–563.

[19] S.H. Lee, A. Gupta, A.D. Compaan, Polycrystalline sputtered Cd(Zn, Mn)Te films for top cells in PV tandem structures, Phys. Status Solidi. 1 (2004) 1042–1045.

[20] P. Mahawela, G. Sivaraman, S. Jeedigunta, J. Gaduputi, M. Ramalingam, S. Subramanian, et al., II–VI compounds as the top absorbers in tandem solar cell structures, Mater. Sci. Eng. B. 116 (2005) 283–291.

[21] N. Amin, A. Yamada, M. Konagai, Effect of ZnTe and CdZnTe alloys at the back contact of 1-μm-thick CdTe thin film solar cells, Japanese J. Appl. Physics, Part 1 Regul. Pap. Short Notes Rev. Pap. 41 (2002) 2834–2841.

[22] A. Morales-Acevedo, Analytical model for the photocurrent of solar cells based on graded band-gap CdZnTe thin films, Sol. Energy Mater. Sol. Cells. 95 (2011) 2837–2841.

[23] A. Aydinli, A. Compaan, G. Contreras-Puente, A. Mason, Polycrystalline $Cd_{1-x}Zn_xTe$ thin films on glass by pulsed laser deposition, Solid State Commun. 80 (1991) 465–468.

[24] K. Prabakar, S. Venkatachalam, Y.L. Jeyachandran, S.K. Narayandass, D. Mangalaraj, Microstructure, Raman and optical studies on $Cd_{0.6}Zn_{0.4}Te$ thin films, Mater. Sci. Eng. B Solid-State Mater. Adv. Technol. 107 (2004) 99–105.

[25] K.R. Murali, Properties of brush plated $Cd_xZn_{1-x}Te$ thin films, Sol. Energy. 82 (2008) 220–225.

[26] H. Zhou, D. Zeng, S. Pan, Effect of Al-induced crystallization on CdZnTe thin films deposited by radio frequency magnetron sputtering, Nucl. Instruments Methods Phys. Res. Sect. A Accel. Spectrometers, Detect. Assoc. Equip. 698 (2013) 81–83.

[27] H. Xu, R. Xu, J. Huang, J. Zhang, K. Tang, L. Wang, The dependence of Zn content on thermal treatments for $Cd_{1-x}Zn_xTe$ thin films deposited by close-spaced sublimation, Appl. Surf. Sci. 305 (2014) 477–480.

[28] J. Huang, L.J. Wang, K. Tang, R. Xu, J.J. Zhang, Y.B. Xia, et al., Growth of High Quality CdZnTe Films by Close-Spaced Sublimation Method, Phys. Procedia. 32 (2012) 161–164.

[29] L. Cai, L. Wang, J. Huang, B. Yao, K. Tang, J. Zhang, et al., Preparation of polycrystalline CdZnTe thick film Schottky diode for ultraviolet detectors, Vacuum. 88 (2013) 28–31.

[30] J. Tao, H. Xu, Y. Zhang, H. Ji, R. Xu, J. Huang, et al., Interface chemistry of CdZnTe films studied by a peel-off approach, Appl. Surf. Sci. (2016) 1–5.

[31] S. Tobeñas, E.M. Larramendi, E. Purón, O. de Melo, F. Cruz-Gandarilla, M. Hesiquio-Garduño, et al., Growth of $Cd_{(1-x)}Zn_xTe$ epitaxial layers by isothermal closed space sublimation, J. Cryst. Growth. 234 (2002) 311–317.

[32] O. de Melo, A. Domínguez, K. Gutiérrez Z-B, G. Contreras-Puente, S. Gallardo-Hernández, A. Escobosa, et al., Graded composition $Cd_xZn_{1-x}Te$ films grown by Isothermal Close Space Sublimation technique, Sol. Energy Mater. Sol. Cells. 138 (2015) 17–21.

[33] M. Levy, N. Amir, E. Khanin, Y. Nemirovsky, R. Beserman, Characterization of CdTe substrates and MOCVD $Cd_{1-x}Zn_xTe$ epilayers, J. Cryst. Growth. 197 (1999) 626–629.

[34] D.J. Olego, P.M. Raccah, J.P. Faurie, Compositional dependence of the Raman frequencies and line shapes of $Cd_{1-x}Zn_xTe$ determined with films grown by molecular-beam epitaxy, Phys. Rev. B. 33 (1986) 3819–3822.

[35] S. Perkowitz, L.S. Kim, Z.C. Feng, P. Becla, Optical phonons in $Cd_{1-x}Zn_xTe$, Phys. Rev. B. 42 (1990) 1455–1457.

[36] M. Schieber, T.E. Schlesinger, R.B. James, H. Hermon, H. Yoon, M. Goorsky, Study of impurity segregation, crystallinity, and detector performance of melt-grown cadmium zinc telluride crystals, J. Cryst. Growth. 237-239 (2002) 2082–2090.

[37] A. Medvid, P. Onufrijevs, A. Mychko, Properties of nanocones formed on a surface of semiconductors by laser radiation: quantum confinement effect of electrons, phonons, and excitons., Nanoscale Res. Lett. 6 (2011) 582.

[38] I. Nasieka, L. Rashkovetskyi, O. Strilchuk, B. Danilchenko, Gamma-stimulated change of the photoluminescence properties of $Cd_{1-x}Zn_xTe$ thin films, Nucl. Instruments Methods Phys. Res. Sect. A Accel. Spectrometers, Detect. Assoc. Equip. 648 (2011) 290–292.

[39] D.J. Olego, J.P. Faurie, S. Sivananthan, P.M. Raccah, Optoelectronic properties of $Cd_{1-x}Zn_xTe$ films grown by molecular beam epitaxy on GaAs substrates, Appl. Phys. Lett. 47 (1985) 1172–1174.

[40] H.C. Poon, Z.C. Feng, Y.P. Feng, M.F. Li, Relativistic band structure of ternary II-VI semiconductor alloys containing Cd, Zn, Se and Te, J. Phys. Condens. Matter. 7 (1995) 2783–2799.

[41] D.N. Talwar, Z.C. Feng, P. Becla, Impurity-induced phonon disordering in $Cd_{1-x}Zn_xTe$ ternary alloys, Phys. Rev. B. 48 (1993) 17064–17071.

[42] A. Medvid', D.V. Korbutyak, S.G. Krylyuk, Y.V. Kryuchenko, E.I. Kuznetsov, I.M. Kupchak, et al., Influence of powerful laser irradiation on impurity-defect structure of CdTe detector material, Nucl. Instruments Methods Phys. Res. Sect. A Accel. Spectrometers, Detect. Assoc. Equip. 531 (2004) 157–160.

[43] V. Kosyak, A. Opanasyuk, P.M. Bukivskij, Y.P. Gnatenko, Study of the structural and photoluminescence properties of CdTe polycrystalline films deposited by close-spaced vacuum sublimation, J. Cryst. Growth. 312 (2010) 1726–1730.

[44] A. S. Opanasyuk, D.I. Kurbatov, V. V. Kosyak, S.I. Kshniakina, S.N. Danilchenko, Characteristics of structure formation in zinc and cadmium chalcogenide films deposited on nonorienting substrates, Crystallogr. Reports. 57 (2012) 927–933.

[45] V. Kosyak, A.I. Opanasyuk, I. Protsenko, C. Panchal, Structural and substructural properties of the zinc and cadmium chalcogenides (review), J. Nano- Electron. Phys. 3 (2011) 274–301.

[46] V. V. Kosyak, M.M. Kolesnyk, A.S. Opanasyuk, Point defect structure in CdTe and ZnTe thin films, J. Mater. Sci. Mater. Electron. 19 (2008) 375–381.

[47] J. Goldstein, D.E. Newbury, D.C. Joy, C.E. Lyman, P. Echlin, E. Lifshin, et al., Scanning Electron Microscopy and X-ray Microanalysis: Third Edition, Springer Science & Business Media, 2012.

[48] D. Kurbatov, A. Opanasyuk, H. Khlyap, Substrate-temperature effect on the microstructural and optical properties of ZnS thin films obtained by close-spaced vacuum sublimation, Phys. Status Solidi Appl. Mater. Sci. 206 (2009) 1549–1557.

[49] D. Kurbatov, V. Kosyak, M. Kolesnyk, A. Opanasyuk, S. Danilchenko, Morfological and structural characteristics of II-VI semiconductor thin films (ZnTe, CdTe, ZnS), Integr. Ferroelectr. 103 (2008) 32–40.

[50] Y.P. Gnatenko, A.S. Opanasyuk, M.M. Ivashchenko, P.M. Bukivskij, I.O. Faryna, Study of the correlation between structural and photoluminescence properties of CdSe thin films deposited by close-spaced vacuum sublimation, Mater. Sci. Semicond. Process. 26 (2014) 663–668.

[51] J.A. Garcia, A. Remon, V. Munoz, R. Triboulet, Annealing-induced changes in the electronic and structural properties of ZnTe substrates, J. Mater. Res. 15 (2000) 1612–1616.

[52] Y.P. Gnatenko, O.A. Shigil'chev, E. Rutkovskii, G. Contreras-Puente, M. Cardenas-Garcia, Photoluminescence and multiphonon resonant Raman scattering in Ni- and Co-doped $Zn_{1-x}Mn_xTe$ crystals, Phys. Solid State. 40 (1998) 564–568.

[53] M.S. Furyer, P.A. Skubenko, P.M. Bukivskij, L.M. Tarakhan, E.D. Chesnokov, I.G. Vertegel, et al., Study of the photoluminescence and photoelectric properties of $Pb_{1-x}Cd_xI_2$ alloys, J. Appl. Phys. 108 (2010) 103711.

[54] Y.P. Gnatenko, M.S. Furyer, A.P. Bukivskii, L.M. Tarakhan, R.V. Gamernyk, Photoluminescence and photoelectric properties of CdTe crystals doped with Er atoms, J. Lumin. 160 (2015) 258–261.

[55] D. Ouadjaout, Y. Marfaing, Localized excitons in II-VI semiconductor alloys: Density-of-states model and photoluminescence line-shape analysis, Phys. Rev. B. 41 (1990) 12096–12105.

[56] L.G. Suslina, D.L. Fedorov, A.G. Areshkin, V.G. Melekhin, Localized excitons and energy transfer in $Zn_xCd_{1-x}S$ solid solutions, Solid State Commun. 55 (1985) 345–349.

[57] S.B. Baranovski, A.L. Efros, Smearing of band edges in solid solutions, Fiz. Techn. Semic. 12 (1978) 2233.

[58] E. Cohen, M.D. Sturge, Fluorescence line narrowing, localized exciton states, and spectral diffusion in the mixed semiconductor CdS_xSe_{1-x}, Phys. Rev. B. 25 (1982) 3828–3840.

[59] M.A. Kanehisa, R.J. Elliott, Effect of disorder on exciton binding in semiconductor alloys, Phys. Rev. B. 35 (1987) 2228–2236.

[60] Y.P. Gnatenko, I.O. Faryna, P.M. Bukivskij, O.A. Shigiltchoff, R. V Gamernyk, S.Y. Paranchych, Nature and energy structure of impurity and intrinsic defects in V-doped $Cd_{1-x}Hg_xTe$, Semicond. Sci. Technol. 20 (2005) 378–388.

[61] J.M. Figueroa, F. Sanchez-Sinencio, J.G. Mendoza-Alvarez, O. Zelaya, C. Vázquez-López, J.S. Helman, Influence of Cd vacancies on the photoluminescence of CdTe, J. Appl. Phys. 60 (1986) 452.

[62] Y.P. Gnatenko, P.M. Bukivskij, I.O. Faryna, A.S. Opanasyuk, M.M. Ivashchenko, Photoluminescence of high optical quality CdSe thin films deposited by close-

spaced vacuum sublimation, J. Lumin. 146 (2014) 174–177.

[63] E. Molva, J.L. Pautrat, K. Saminadayar, G. Milchberg, N. Magnea, Acceptor states in CdTe and comparison with ZnTe. General trends, Phys. Rev. B. 30 (1984) 3344–3354.

[64] J.M. Francou, K. Saminadayar, J.L. Pautrat, Shallow donors in CdTe, Phys. Rev. B. 41 (1990) 12035–12046.

[65] A. Castaldini, A. Cavallini, B. Fraboni, P. Fernandez, J. Piqueras, Deep energy levels in CdTe and CdZnTe, J. Appl. Phys. 83 (1998) 2121.

[66] S. Seto, A. Tanaka, F. Takeda, K. Matsuura, Defect-induced emission band in CdTe, J. Cryst. Growth. 138 (1994) 346–351.

[67] S. Hildebrandt, H. Uniewski, J. Schreiber, H.S. Leipner, Localization of Y Luminescence at Glide Dislocations in Cadmium Telluride, J. Phys. III. 7 (1997) 1505–1514.

[68] V. Babentsov, J. Franc, P. Höschl, M. Fiederle, K.W. Benz, N. V. Sochinskii, et al., Characterization of compensation and trapping in CdTe and CdZnTe: Recent advances, Cryst. Res. Technol. 44 (2009) 1054–1058.

[69] J. Aguilar Hernandez, M. Cardenas Garcia, G. Contreras Puente, J. Vidallarramendi, Analysis of the 1.55 eV PL band of CdTe polycrystalline films, Mater. Sci. Eng. B. 102 (2003) 203–206.

[70] Y.P. Gnatenko, P.M. Bukivskij, A.S. Opanasyuk, D.I. Kurbatov, M.M. Kolesnyk, V.V. Kosyak, et al., Low-temperature photoluminescence of II-VI films obtained by close-spaced vacuum sublimation, J. Lumin. 132 (2012) 2885–2888.

[71] J.F. Scott, R.C.C. Leite, T.C. Damen, Resonant Raman Effect in Semiconductors, Phys. Rev. 188 (1969) 1285–1290.

[72] S. Adachi, Properties of Group-IV, III-V and II-VI Semiconductors, John Wiley & Sons, 2005.

[73] D. Nam, H.Cheong, A.S.Opanasyuk, P.V.Koval, V.V.Kosyak, P.M.Fochuk, Raman investigation on thin and thick CdTe films obtained by close spaced vacuum sublimation technique, Phys. Status Solidi. 4 (2014) 1–4.

[74] Z.C. Feng, S. Perkowitz, J.M. Wrobel, J.J. Dubowski, Outgoing multiphonon resonant Raman scattering and luminescence near the $E_0 + \Delta_0$ gap in epitaxial CdTe films, Phys. Rev. B. 39 (1989) 12997–13000.

[75] Y.L. Wu, Y.-T. Chen, Z.C. Feng, J.-F. Lee, P. Becla, W. Lu, Synchrotron radiation x-ray absorption fine-structure and Raman studies on CdZnTe ternary alloys, Hard X-Ray, Gamma-Ray, Neutron Detect. Phys. XI. 7449 (2009) 74490Q–11.

[76] P.M. Amirtharaj, F.H. Pollak, Raman scattering study of the properties and removal of excess Te on CdTe surfaces, Appl. Phys. Lett. 45 (1984) 789–791.

[77] S. A. Hawkins, E. Villa-Aleman, M.C. Duff, D.B. Hunter, A. Burger, M. Groza, et al., Light-induced tellurium enrichment on CdZnTe crystal surfaces detected by Raman spectroscopy, J. Electron. Mater. 37 (2008) 1438–1443.

[78] L.C. Teague, S. A. Hawkins, M.C. Duff, M. Groza, V. Buliga, A. Burger, AFM characterization of raman laser-induced damage on CdZnTe crystal surfaces, J. Electron. Mater. 38 (2009) 1522–1527.

[79] J.C. Irwin, J. Lacombe, Raman scattering in ZnTe, J. Appl. Phys. 41 (1970) 1444–1450.

Table 1 The parameters of samples obtained from XRD, PL and Raman study

Samples	Ratio of CdTe to ZnTe powder (M_R)	Zn concentration, x		XRD analysis				E_g (4.5 K), eV	Raman shift LO_2, cm^{-1}
		XRD	EDS	Lattice parameter, nm	FWHM (111), degrees	CSD size, nm	MS $\times 10^{-3}$		
CdTe	-	0	-	0.6494	0.13	74.0	2.53	1.606	-
CZT1	8	0.10	0.13	0.6441	0.20	47.8	3.89	1.668	177.5
CZT2	4	0.32	0.40	0.6359	0.28	33.1	5.54	1.842	190.2
CZT3	3	0.44	0.49	0.6316	0.37	25.3	7.22	1.996	197.4
CZT4	2	0.67	0.64	0.6232	0.68	13.5	13.30	2.150	200.8
ZnTe	-	1	-	0.6110	0.10	99.2	1.78	2.395	205.6

Fig. 1 SEM images of CZT samples surface: (a) CZT1, (b) CZT2, (c) CZT3, (d) CZT4.

Fig.2 XRD patterns of CdTe, CZT1, CZT2, CZT3, CZT4 and ZnTe samples.

Fig. 3 PL spectra of the samples: CdTe (a), CZT1 (b), CZT2 (c), CZT3 (d), CZT4 (e) and ZnTe (f) measured at 4.5 K.

Fig. 4 Room temperature Raman spectra of the Te crystal measured with 514 (a), 633 (b) and 785 nm (c) excitation.

Fig. 5 Room temperature Raman spectra of the CdTe film measured with 514 (a), 633 (b) and 785 nm (c) excitation.

Fig. 6 Room temperature Raman spectra of the CdTe and CZT1 measured with 785 nm excitation, as well as CZT2, CZT3, CZT4 and ZnTe films measured with 633 nm excitation.

Fig. 1

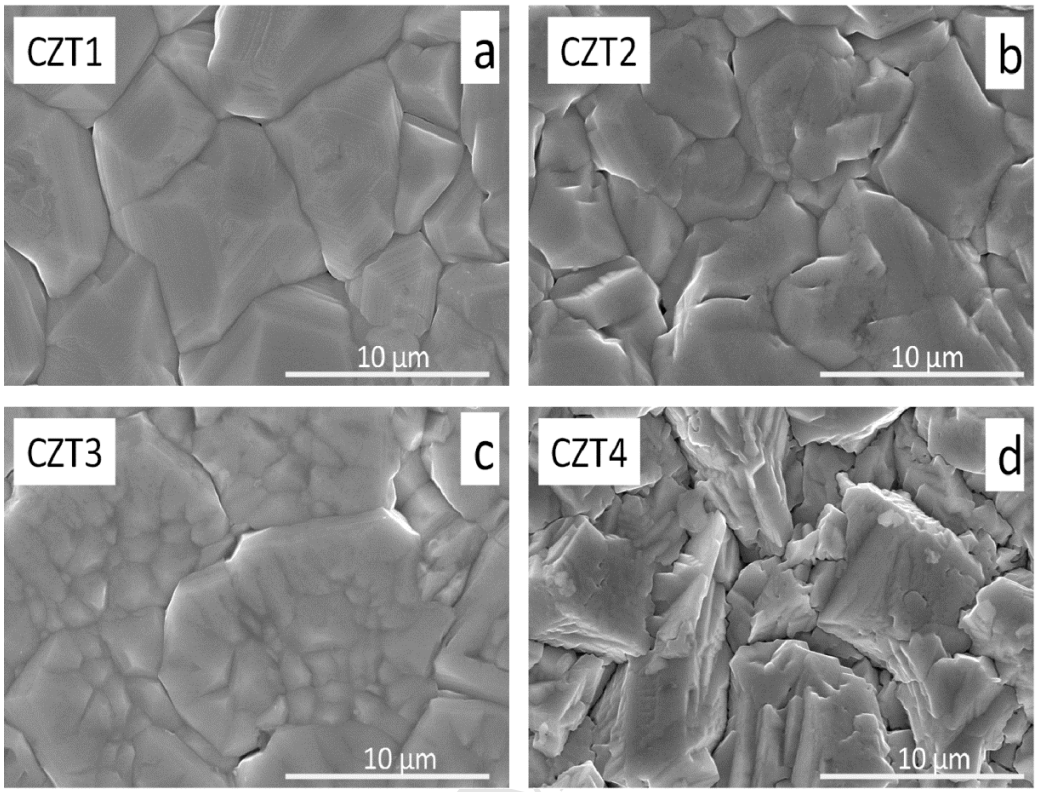

Fig.2

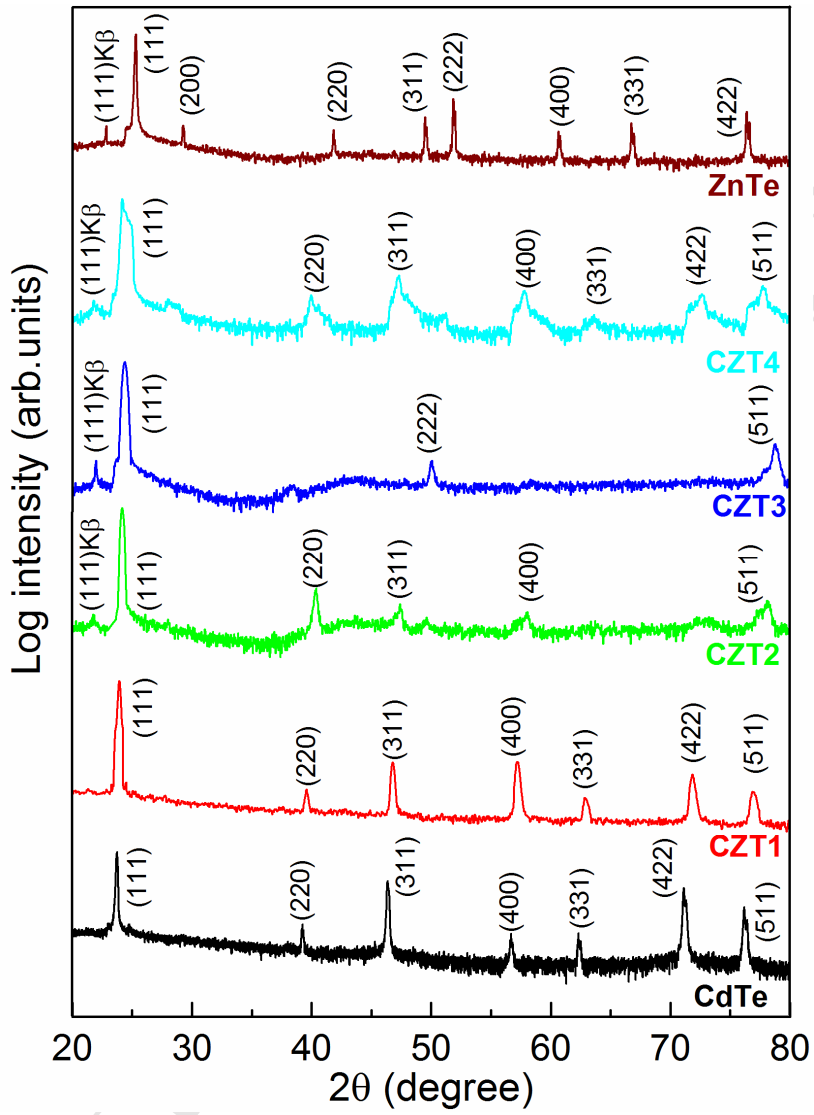
Log intensity (arb.units)
2θ (degree)
20
30
40
50
60
70
80
ZnTe
(111)Kβ
(111)
(200)
(220)
(311)
(222)
(400)
(331)
(422)
CZT4
(111)Kβ
(111)
(220)
(311)
(400)
(331)
(422)
(511)
CZT3
(111)Kβ
(111)
(222)
(511)
CZT2
(111)Kβ
(111)
(220)
(311)
(400)
(511)
CZT1
(111)
(220)
(311)
(400)
(331)
(422)
(511)
CdTe
(111)
(220)
(311)
(400)
(331)
(422)
(511)

Fig. 3

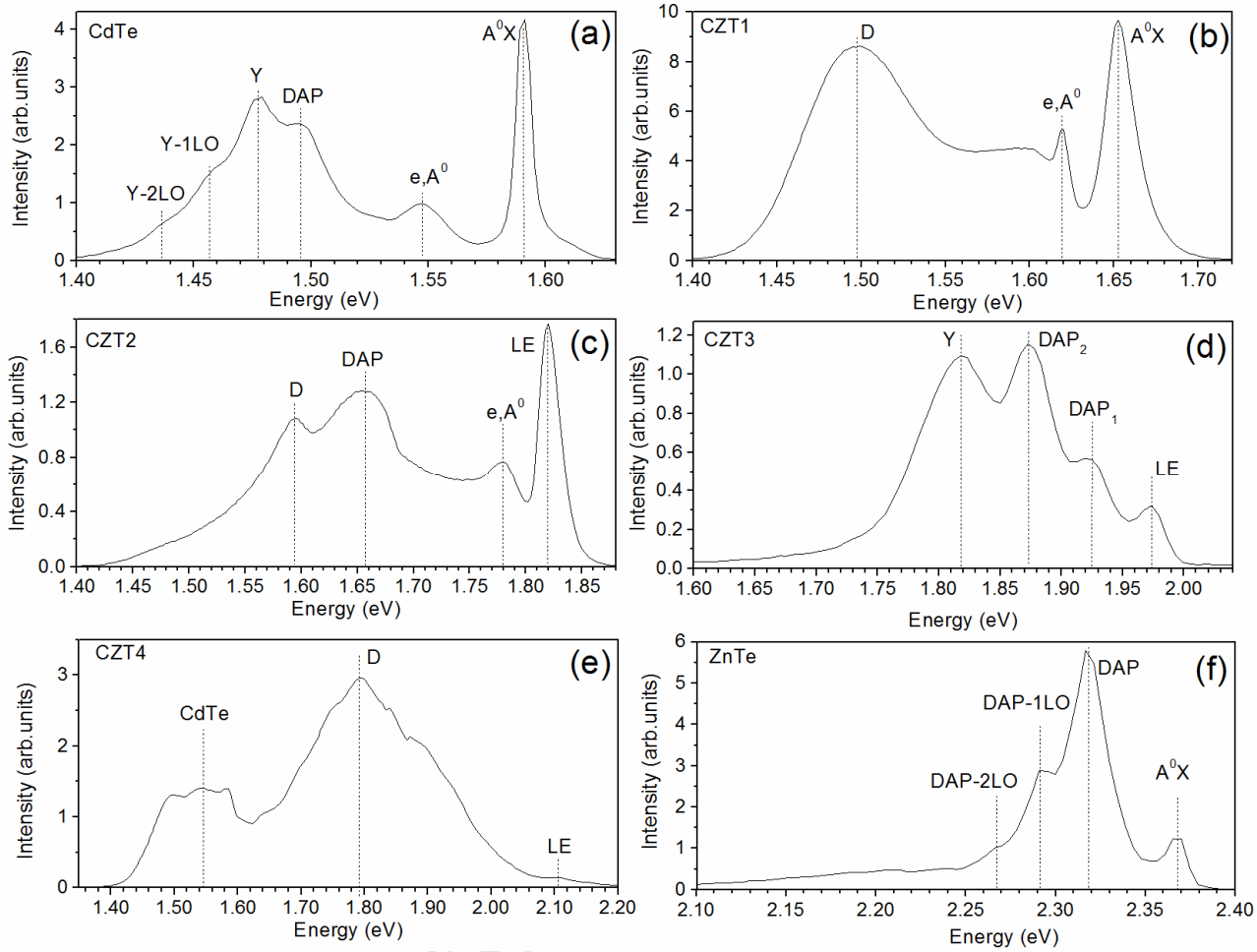

Fig. 4

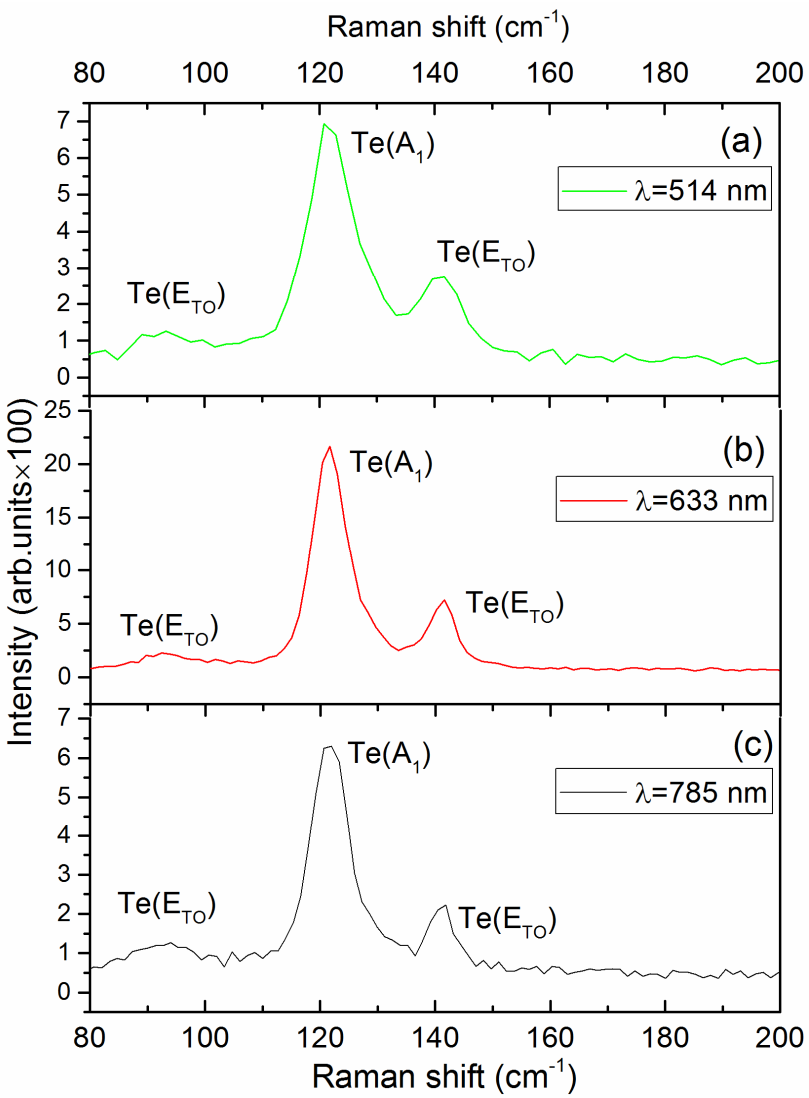
Raman shift (cm-1)
80
100
120
140
160
180
200
Intensity (arb.units×100)
(a)
λ=514 nm
Te(A1)
Te(ETO)
Te(ETO)
(b)
λ=633 nm
Te(A1)
Te(ETO)
Te(ETO)
(c)
λ=785 nm
Te(A1)
Te(ETO)
Te(ETO)
Raman shift (cm-1)

Fig. 5

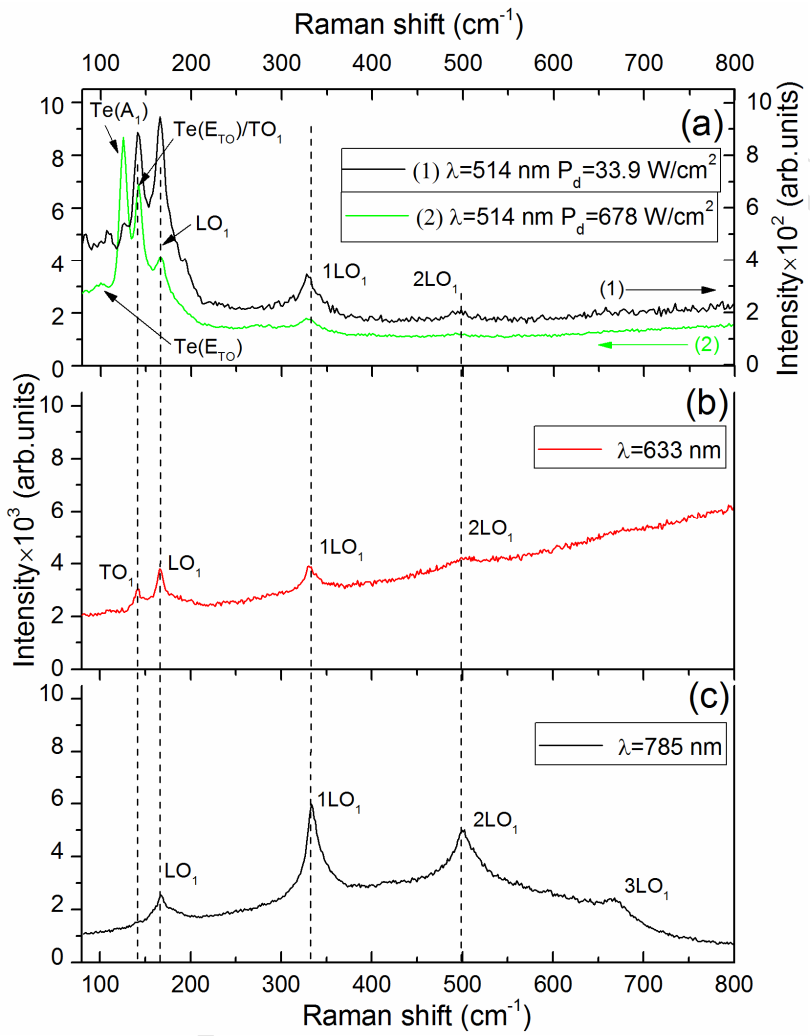
Raman shift (cm-1)
100
200
300
400
500
600
700
800
(a)
Te(A1)
Te(ETO)/TO1
LO1
1LO1
2LO1
(1)
(2)
Te(ETO)
(1) λ=514 nm Pd=33.9 W/cm2
(2) λ=514 nm Pd=678 W/cm2
Intensity×10-2 (arb.units)
(b)
λ=633 nm
TO1
LO1
1LO1
2LO1
Intensity×10-3 (arb.units)
(c)
λ=785 nm
LO1
1LO1
2LO1
3LO1
Raman shift (cm-1)

Fig. 6

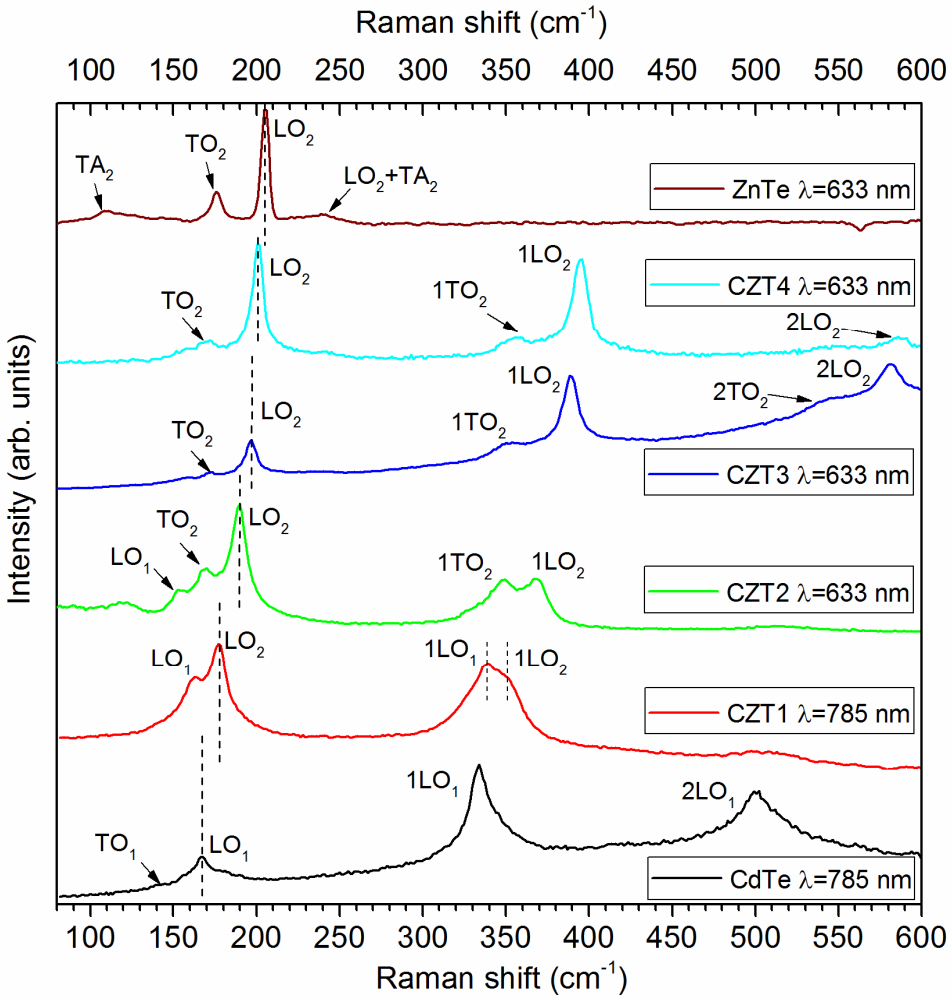
Raman shift (cm-1)
100 150 200 250 300 350 400 450 500 550 600
Intensity (arb. units)
TA2
TO2
LO2
LO2+TA2
ZnTe λ=633 nm
1LO2
1TO2
2LO2
CZT4 λ=633 nm
2TO2
CZT3 λ=633 nm
LO1
CZT2 λ=633 nm
1LO1
CZT1 λ=785 nm
TO1
CdTe λ=785 nm

- New approach for deposition of $Cd_{1-x}Zn_xTe$ thick films has been developed.
- Effect of chemical composition on $Cd_{1-x}Zn_xTe$ thick films properties was studied.
- The proposed approach allows obtaining of high-quality $Cd_{1-x}Zn_xTe$ thick films.
- Compositional dependence of Raman modes friquencies was established.